ELSEVIER

Ceramics International 31 (2005) 287–291

CERAMICS INTERNATIONAL

www.elsevier.com/locate/ceramint

Varistor properties of Sc_2O_3-doped Sn·Co·Nb ceramics

Wen-Xin Wang[a], Jin-Feng Wang[a,*], Hong-Cun Chen[a], Wen-Bin Su[a], Bin Jiang[b], Guo-Zhong Zang[a], Chun-Ming Wang[a], Peng Qi[a]

[a]*School of Physics and Microelectronics, National Key Laboratory of Crystal Materials, Shandong University, Jinan 250100, PR China*
[b]*Department of Physics and Astronomy, Arizona State University, Tempe, AZ 85287-1054, USA*

Received 22 January 2004; received in revised form 19 March 2004; accepted 3 May 2004
Available online 21 August 2004

Abstract

The varistor properties of Sc_2O_3-doped SnO_2·Co_2O_3·Nb_2O_5 ceramics were investigated. It was found that the non-linear coefficient presents a peak of 17.1 at the concentration of 0.06 mol% Sc_2O_3, the average grain size decreases from 10 to 5 μm, the breakdown electrical field increases from 199 to 1790 V/mm and relative electrical permittivity decreases from 2600 to 60 as Sc_2O_3 concentration was increased up to 0.09 mol%. The increase of the breakdown electrical field with increasing Sc_2O_3 concentration is mainly attributed to the decrease of the average grain size. The reason why the permittivity decreases with increasing Sc_2O_3 concentration was originated from the ratio of the grain size to the barrier width. To illustrate the grain-boundary barrier formation of (Sc, Co, Nb)-doped SnO_2 varistors, a modified defect barrier model was introduced, in which the negatively charged acceptors substituting for Sn ions should be located at SnO_2 lattice sites in the depletion layers, instead at the grain interfaces.

PACS: 72.20.Ht

Keywords: B. Grain boundaries; C. Electrical properties; E. Varistors

1. Introduction

Varistors can sense and limit high transient voltage surges and can repeatedly endure such surges without being destroyed. For this reason, they are usually used to protect electronic circuits from voltage pulse shock. The most important property of a varistor is its non-linear voltage–current characteristic. It can be expressed by equation $I = KV^{\alpha}$, where α is non-linear coefficient, the essential parameter to scale the non-linearity.

Currently, widely used varistor is ZnO varistor, because of its high non-linear coefficients [1], but the degradation problem of ZnO varistors has not been resolved. Therefore, the efforts to search new varistor materials have not been interrupted. In 1995, S.A. Pianaro found a new varistor material [2] (Co, Nb)-doped SnO_2, which has only single phase, rutile structure. The high densification of the SnO_2 ceramics is attributed to the cobalt effect in the SnO_2 lattice. In this work, the properties of Sc_2O_3-doped SnO_2·Co_2O_3·Nb_2O_5 varistors were investigated, and some new results were obtained.

2. Experiments and measurements

The raw chemicals were analytic grades of SnO_2 (99.5%), Co_2O_3(99%), Nb_2O_5(99.5%), and Sc_2O_3(99.27%). The compositions were $(99.15-x)\%SnO_2 + 0.75\%Co_2O_3 + 0.10\%Nb_2O_5 + x\%Sc_2O_3$ in molar system, where x = 0.00, 0.03, 0.06, 0.09. Varistors were prepared by conventional ceramic processing. The mixed raw chemicals were milled in nylon kettle with ZrO_2 balls and some distilled water, dried, mixed with 0.5% weight of polyvinyl alcohol (PVA) binder and pressed into disks 15 mm in diameter and 1.5 mm in thickness at 180 MPa. After being burned out the PVA binder

* Corresponding author. Tel.: +86 531 856 7851; Fax: +86 531 837 7031.
E-mail address: wangjf@sdu.edu.cn (J.-F. Wang).

0272-8842/$30.00
doi:10.1016/j.ceramint.2004.05.018

at 650 °C, the disks were sintered at 1350 °C for an hour and cooled freely to room temperature.

For microstructure characterization, the samples were analyzed by scanning electron microscope (SEM), The mean grain sizes were determined by the intercept method. The sample with 0.09 mol% Sc_2O_3 was analyzed by high-resolution transmission electron microscope (HRTEM). Beforehand, the sample for HRTEM was polished on both sides and thinned to less than 1 μm with ion beam thinner. For electrical characterization of current density versus applied electrical field, an *I–V* grapher (QT2) was used. The dependence of permittivity on frequency was determined with Agilent 4294A impedance analyzer in the frequency range 40 Hz–15 MHz.

The non-linear coefficient α is calculated by the following equation [1,3]:

$$\alpha = \frac{\log(I_2/I_1)}{\log(V_2/V_1)} \tag{1}$$

where I_2 and I_1 ($I_2 > I_1$) are prescriptive currents 10 mA and 1 mA, V_2 and V_1 are the voltages at currents I_2 and I_1, respectively. The field at current 1 mA was chosen as the breakdown electrical field E_B.

A Schottky-type barrier model is usually used to explain the behavior of varistors [3–9]. According to the model, the current density through a varistor is

$$J_S = AT^2 \exp\left[\frac{\beta\sqrt{E} - \phi_B}{k_B T}\right] \tag{2}$$

where A is Richardson constant, k_B the Boltzman constant, ϕ_B the barrier height, E the electrical field, and β is a constant expressed by the relation

$$\beta \propto \sqrt{\frac{1}{n\omega}} \tag{3}$$

where n is the grain number per unit length and ω the barrier width.

The potential barrier height at grain boundaries is determined by the following approach. In order to remove the influence of electric field on the barrier height [10], J and E of a sample were measured at different temperature. Plots of ln J versus $E^{1/2}$ of a sample were plotted and extrapolated to $E = 0$ to get the intercepts ln J_0. Then, the ln J_0 was plotted versus $1/T$ and the value of ϕ_B can be determined by the slope of the plot. The constant β was obtained by the slope of the plot of ln J versus $E^{1/2}$ at room temperature.

3. Results and discussion

Fig. 1 shows the electrical non-linear characteristics of the samples with different concentration of Sc_2O_3. From Fig. 1 we can see that all samples have good electrical non-linearity. Fig. 2 shows the dependences of α and E_B on the contents of Sc_2O_3. The non-linear coefficient α presents a

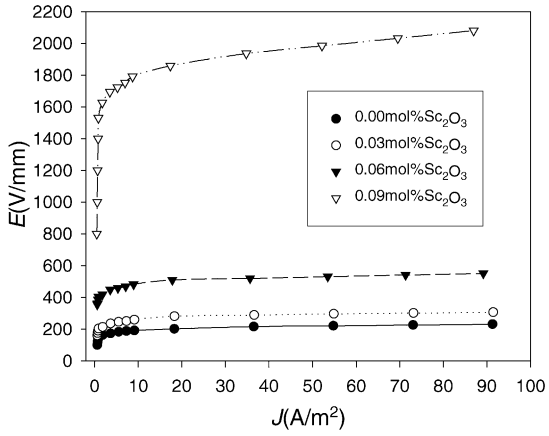

Fig. 1. *J–E* characteristics of samples with different Sc_2O_3 contents.

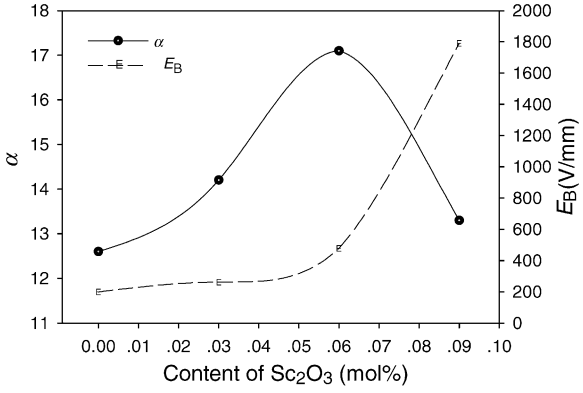

Fig. 2. Non-linear coefficient and breakdown voltage of the samples.

peak (17.1) at 0.06 mol% Sc_2O_3 concentration and the breakdown electrical field monotonously increases with increasing Sc_2O_3 dopants.

The SEM micrographs are presented in Fig. 3. It is clearly shown that the average grain size decreases with increasing Sc_2O_3 dopants. The reason for the breakdown field to

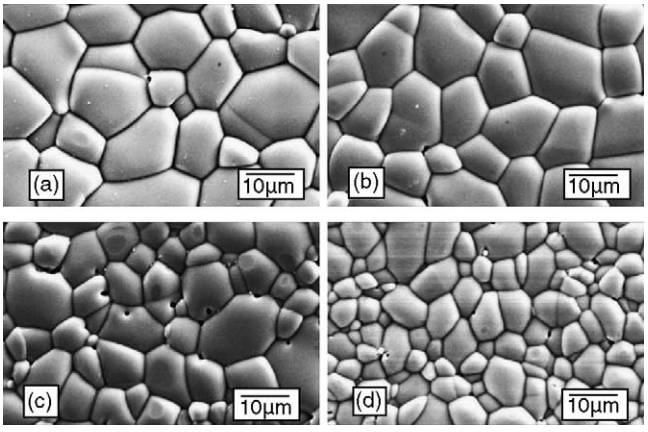

Fig. 3. SEM pictures of different Sc_2O_3 contents: (a) 0.00%; (b) 0.03%; (c) 0.06%; and (d) 0.09%.

Table 1
Characteristics of the samples doped with different contents of Sc_2O_3

Sc_2O_3 (mol%)	α	E_B (V/mm)	Φ_B (eV)	1000β ($em^{0.5}V^{0.5}$)	ε_r[a]	Grain size (μm)	Relative density (%)[b]
0.00	12.6	199	0.58	42	2600	10	97.4
0.03	14.2	262	0.60	35	2000	9	97.3
0.06	17.1	478	0.68	34	1000	7	97.3
0.09	13.3	1790	0.70	19	60	5	97.3

[a] ε_r is measured at 1 kHz.
[b] Theoretical density of SnO_2 is 6950 kg m^{-3}.

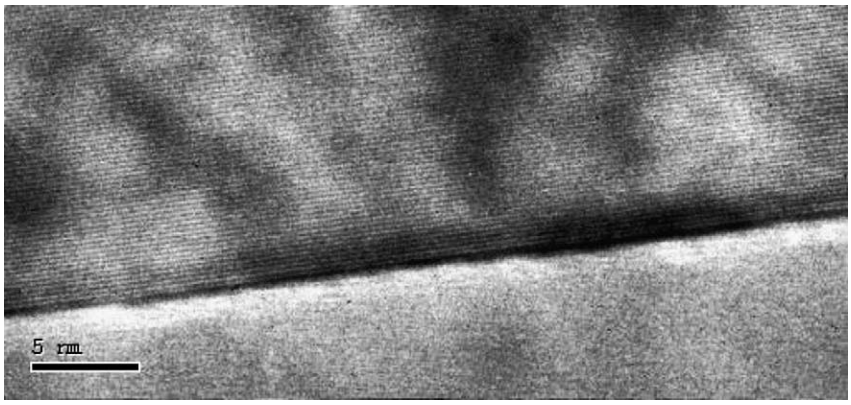

Fig. 4. HRTEM picture of the sample with 0.09 mol% Sc_2O_3.

increase with increasing Sc_2O_3 concentration can be explained according to the equation

$$E_B = nV_{gb} \quad (4)$$

where n is the average grain number per unit length, V_{gb}, about 2.2–3 V [11,12], is the breakdown voltage of a grain boundary. With increasing Sc_2O_3 concentration, the mean grain size decrease significantly, which results in the increase of n. That is the origin why the breakdown field to increase with increasing Sc_2O_3 concentration.

Table 1 shows the variations of non-linear coefficient (α), non-linear electrical field (E_B), permittivities (ε_r), relative density and average grain size of the samples with different contents of Sc_2O_3. All samples have very high and almost the same relative densities. The high densities of the samples can be explained by the close contact of the grains, which is showed in Figs. 3 and 4. Fig. 4 presents a 430K magnified photo of a grain boundary taken by HRTEM. From Fig. 4, we can see that the crystal planes, parallel to the boundary line, of the upper grain extend continuously to the boundary. That is to say that the boundary layer of SnO_2 varistor ceramics does not exist almost.

Fig. 5 shows the plots of the permittivities (ε_r) versus frequency of the samples with different Sc_2O_3 concentrations. It is very clear that the relative permittivity of the varistor system decreases substantially with increasing Sc_2O_3 concentration. The permittivities of all samples are much higher than that (9.65) of SnO_2 crystal. Why the permittivities of all samples are much higher than that of SnO_2 and the relative permittivity of the varistor system decreases substantially with increasing Sc_2O_3 concentration can be explained by following equation [7]:

$$\varepsilon_r = \varepsilon_B \frac{d}{t_B} \quad (5)$$

where ε_B is the internal permittivity of the barrier material, d the mean size of the grain size, and t_B the mean thickness of the boundary barrier. Because, d is larger than t_B and ε_B of the barrier region having a high polarization is greater than ε_r, therefore the permittivities of all samples are much higher than that of SnO_2 crystal. Owing to the significantly decrease of the grain size d of the varistor ceramics with increasing Sc_2O_3 concentration, the relative permittivity of the varistor ceramics decreases greatly with increasing Sc_2O_3 concentration.

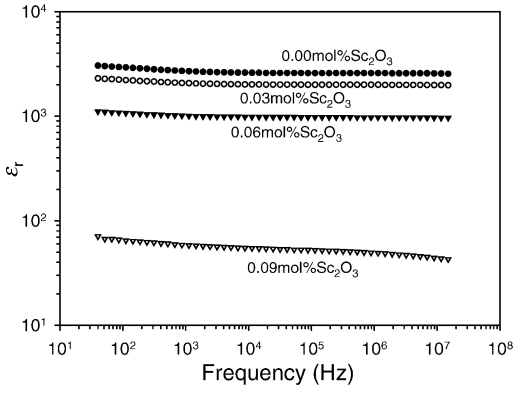

Fig. 5. Permittivity vs. frequency for samples with various Sc_2O_3 contents.

From the fact that the SnO_2 varistors have only single phase with X-ray precision [2,13], one can deduce that the dopants should be mostly dissolved into SnO_2 lattice. The addition of Nb_2O_5 to the SnO_2 ceramics causes an increase of electrical conductivity because of giving off electrons according to the reaction:

$$Nb_2O_5 \xrightarrow{SnO_2} 2Nb_{Sn}^{+} + 2e^{-} + 4O_O + \tfrac{1}{2}O_2 \uparrow \quad (6)$$

where $e^{-}$is an electron activated from donor Nb in the SnO_2 lattice. As a current carrier, the electron elevates the Fermi level of the grains, and thus, heightens the grain boundary barrier.

At high temperature, Co_2O_3 will be decomposed into CoO [14]:

$$Co_2O_3 \xrightarrow{950^{\circ}C} 2CoO + \tfrac{1}{2}O_2 \uparrow \quad (7)$$

The CoO will lead to the reaction

$$CoO \xrightarrow{SnO_2} Co_{Sn}^{2-} + V_O^{2+} + O_O \quad (8)$$

The oxygen vacancies, V_O^{2+}, can speed up defects transportation, which facilitates the SnO_2 grain mergence and raises ceramics density.

Similarly, the addition of Sc_2O_3 to the SnO_2 lattice will lead to the substitution of Sc for Sn according to the following equation:

$$Sc_2O_3 \xrightarrow{SnO_2} 2Sc_{Sn}^{-} + V_O^{2+} + 3O_O \quad (9)$$

Because the radius of Sc^{3+} (81 pm) is much larger than that of Sn^{4+} (71 pm), the addition of Sc_2O_3 will cause SnO_2 lattice to be distorted. That is, the reaction of Eq. (9) is less likely to proceed than the reactions of Eqs. (6) and (8), because the reaction of Eq. (9) should be more energetic than the reactions of Eq. (6) or (8). For this reason, much more Sc_2O_3 will not be combined into SnO_2 lattice instead remaining at SnO_2 grains boundaries. Sc_2O_3 residing at SnO_2 grains boundaries or some compounds of Sc_2O_3 combining with SnO_2 hinder SnO_2 grains from conglomerating. That may be the reason why the grain size of the SnO_2-based varistors decreased significantly with increasing Sc_2O_3 concentration.

Oxygen in the above Eqs. (6) and (7) will be partly absorbed at SnO_2 grain boundaries

$$O_2 \rightarrow 2O_{ad}^{x} \quad (10)$$

The absorbed oxygen capture electrons to become negatively charged O^{-} or O^{2-} [4,6,12].

A grain boundary defect model to explain the formation of Schottky barrier was proposed by Gupta and Carlson [5], for multiphase ZnO varistors. Considering the single phase of SnO_2-based ceramics, Bueno et al [4] developed the model to fit the case of SnO_2 varistors. In the model the negatively charged acceptors substituting for Sn locate at SnO_2 grain interfaces. But, from Eqs. (8) and (9), it can be seen that the negatively charged acceptors substituting for Sn should locate at SnO_2 lattice sites. This deduction is also supported by the fact that a new phase precipitation in the grain boundary is not detected [2,4,9,10]. It appears to us that the defect barrier model should be modified as Fig. 6. Since, a new phase precipitation in the grain boundary is not detected, the two barrier tops should touch each other. In Fig. 6, the positive charged donors (V_O^{2+}, Nb_{Sn}^{+}) expanding from both sides of a grain boundary to the region near the grain boundaries compensate the negative charged acceptors (O^{-}, O^{2-}) at the grain boundary interface. The role of the oxygen in the formation of boundary barriers can be confirmed by impedance analysis [4] and conducting heat treatment for the varistors sintered at oxidizing and reducing atmospheres [12,15]. The Schottky barrier is formed with the depletion layer of width ω.

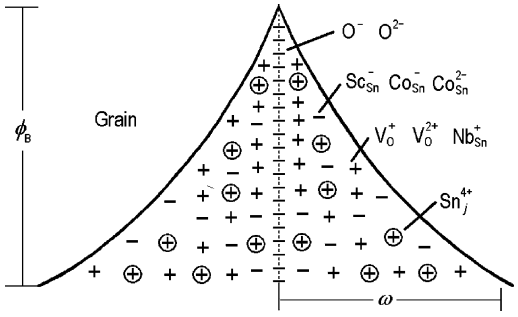

Fig. 6. The grain boundary defect model for Sc_2O_3-doped SnO_2·Co_2O_3·Nb_2O_5.

4. Conclusions

A high non-linear coefficient of 17.1 for the SnO_2 varistor doped with 0.06 mol% Sc_2O_3 was obtained. For the samples sintered at 1350 °C, the deviation either higher or lower off the 0.06 mol% Sc_2O_3 concentration results in the deterioration of the non-linear characteristics. The increase of the breakdown electrical field with increasing Sc_2O_3 concentration is mainly attributed to the decrease of the average grain size. The reason why the permittivity decreases with increasing Sc_2O_3 concentration originates from Sc_2O_3, residing at boundaries, hindering SnO_2 grains from conglomerating.

Acknowledgement

This work is supported by Natural Science Foundation of Shandong Province, China under the Grant No. Z2003F04.

References

[1] T.K. Gupta, J. Am. Ceram. Soc. 73 (1990) 1817–1840.
[2] S.A. Pianaro, P.R. Bueno, E. Longo, J.A. Varela, J. Mater. Sci. Lett. 14 (1995) 692–694.

[3] J.F. Wang, Chin. Phys. Lett. 17 (2000) 530–534.
[4] P.R. Bueno, S.A. Pianaro, E.C. Pereira, et al. J. Appl. Phys. 84 (1998) 3700–3705.
[5] T.K. Gupta, W.G. Carlson, J. Mater. Sci. 20 (1985) 3487–3500.
[6] E.R. Leite, J.A. Varela, E. Longo, J. Mater. Sci. 27 (1992) 5325–5329.
[7] P.R. Emtage, J. Appl. Phys. 48 (1977) 4372–4384.
[8] J.D. Santos, E. Longo, E.R. Leite, J.A. Varela, J. Mater. Res. 13 (1998) 1152–1157.
[9] A.C. Antunes, S.R.M. Antunes, M.R. Rocha, E. Logo, J.A. Varela, J. Mater. Sci. Lett. 17 (1998) 577–579.
[10] S.A. Pianaro, P.R. Bueno, P. Olivi, E. Longo, J.A. Varela, J. Mater. Sci. Lett. 16 (1997) 634–638.
[11] J. Wong, J. Appl. Phys. 47 (1976) 4971–4974.
[12] E.R. Leite, A.M. Nascimento, P.R. Bueno, E. Longo, J.A. Varela, J. Mater. Sci.: Mater. Electr. 10 (1999) 321–327.
[13] S.A. Pianaro, P.R. Bueno, E. Longo, J.A. Varela, Ceram. Int. 25 (1999) 1–6.
[14] J.A. Cerri, E.R. Leite, D. Gouvea, E. Longo, J.A. Varela, J. Am. Ceram. Soc. 79 (1996) 799–804.
[15] M.R.C. Santos, P.R. Bueno, E. Longo, J.A. Varela, J. Eur. Ceram. Soc. 21 (2001) 161–167.